**Moroccan Journal of Chemistry**
**ISSN : 2351-812X**


**Mor. J. Chem., 2023, Volume 11, Issue 4, Page 1254-1265**
https://revues.imist.ma/index.php/morjchem
https://doi.org/10.48317/IMIST.PRSM/morjchem-v11i04.41366

# First-principles investigation of electronic, elastic, optical and thermoelectric properties of strontium-based anti-perovskite $Sr_3MN$ (M= P and As) for potential applications in optoelectronic and thermoelectric devices

**Bouhmaidi S. [1*], Pingak R. K. [2], Setti L. [1**]**
*[1]Laboratory of Advanced Science and Technologies, FPL, Abdelmalek Essaadi University, Tetouan, Morocco*
*[2]Department of Physics, Faculty of Sciences and Engineering, University of Nusa Cendana, Kupang, 85001, Indonesia*
**Corresponding author, Email address: soukaina.bouhmaidi@etu.uae.ac.ma*
***Corresponding author, Email address: settilarbi@gmail.com*

***Received*** *09 July 2023,*
***Revised*** *09 Sept 2023,*
***Accepted*** *19 Sept 2023*

***Citation:*** *Bouhmaidi S., Pingak R. K., Setti L. (2023) First-principles investigation of electronic, elastic, optical and thermoelectric properties of strontium-based anti-perovskite $Sr_3MN$ (M = P and As) for potential applications in optoelectronic and thermoelectric devices, Mor. J. Chem., 11(4), 1254-1265*

**Abstract:** This work aims to study the electronic, elastic, optical and thermoelectric properties of the cubic $Sr_3MN$ (M=P and As) anti-perovskites. The properties of the cubic $Sr_3PN$ are investigated for the first time in this work while those of the $Sr_3AsN$ are compared with other theoretical results in the literature. The Density Functional Theory (DFT) implemented in the Quantum Espresso (QE) package with the GGA-PBE functional was used throughout this study. $Sr_3PN$ and $Sr_3AsN$ were found to be chemically and mechanically stable with optimized lattice parameters of 5.07 Å and 5.11 Å, respectively. Results also showed that the two compounds are p-type semiconductors with direct band gaps of 0.56 eV and 0.45 eV for the respective compounds. The materials are also predicted to have exceptional optical properties including high absorption in the order of $10^5$ $cm^{-1}$ in the visible and ultraviolet region and hence are promising optoelectronic materials. Moreover, the calculated thermoelectric properties of the two materials strongly suggest that the two materials are potential for thermoelectric applications.

**Keywords:** Anti-perovskite $Sr_3MN$; DFT; Optoelectronic properties; Thermoelectric properties

## 1. Introduction

A large number of recent studies (Song *et al.*, 2023; Song *et al.*, 2022; Bouhmaidi *et al.*, 2023; Bouhmaidi *et al.*, 2022; Nguyen *et al.*, 2022; Pingak, 2022; Pingak *et al.*, 2023; Roknuzzaman *et al.*, 2017; Bouhmaidi *et al.*, 2022; Pingak *et al.*, 2022; Ho-Baillie *et al.*, 2021; Huang *et al.*, 2021; Aman *et al.*, 2018) have demonstrated that perovskites with general formula $ABX_3$ possess outstanding properties, making them promising for applications in optoelectronic and thermoelectric devices. Similar results were also reported for a large number of double perovskites (Harbi and Moutaabbid, 2022; Behera and Mukherjee, 2022; Harbi *et al.*, 2019; Hassan *et al.* 2018). Within such materials, A and B are cations and X is the anion.

Recently, anti-perovskite materials with formula $X_3AB$ have also been found as promising materials for various applications due to their attractive physical properties. The anti-perovskite is a

derivative of the electron reversal of the perovskite, with the positive and negative ions occupying opposite positions: the ions at positions A and B of the perovskites (anti-perovskites) are cations (anions), and the ions at position X are anions (cations) (Li *et al.*, 2023). Some of their interesting properties include semiconductivity (Mochizuki *et al.*, 2020), outstanding optoelectronic and photovoltaic properties (Liang *et al.*, 2022; Oyeniyi, 2022; Dahbi *et al.*, 2022; Kadri *et al.*, 2023), thermoelectricity (Okamoto *et al.*, 2016; Hassan *et al.*, 2018), superconductivity (He *et al.*, 2013; Oudah *et al.*, 2016), and ferromagnetism (Zhang *et al.*, 2012).

In particular, anti-perovskite nitrides possess remarkable properties and have been a focus of some recent studies. Beznosikov (Beznosikov, 2003) carried out a crystal and chemical analysis of the structures of perovskite-like nitrides and he predicted more than 80 new nitrides with anti-perovskite structure. Recently, Behera and co-workers (Behera *et al.*, 2022) demonstrated that $Mg_3NX$ (X = Ge, Sn) anti-perovskites are metallic in nature as well as mechanically and dynamically stable, making them promising for various applications.

Due to its excellent optoelectronic and thermoelectric properties, $Sr_3AsN$ anti-perovskite has been intensively studied by a number of studies (Mochizuki *et al.*, 2020; Farid *et al.*, 2021; Haque and Hossain, 2019; Ullah *et al.*, 2016; Hichour *et al.*, 2010; Haddadi *et al.*, 2009). The studies have reported that the $Sr_3AsN$ anti-perovskite is a promising optoelectronic and thermoelectric material. However, most of the studies focused on its optoelectronic and elastic properties, only a few (Farid *et al.*, 2021; Haque and Hossain, 2019) studied its thermoelectric properties. On the other hand, $Sr_3PN$ anti-perovskite, which is an isoelectronic form of $Sr_3AsN$, has been rarely studied. Investigations on $Sr_3PN$ anti-perovskite have been reported in Refs (Mochizuki *et al.*, 2020; Sreedevi *et al.*, 2022), focusing only on its optoelectronic properties. To the best of our knowledge, the thermoelectric properties of the compound have not been reported.

To evaluate the potential of strontium based anti-perovskites $Sr_3AsN$ and $Sr_3PN$ in optoelectronic and thermoelectric devices, a comprehensive study on their optoelectronic, elastic, and thermoelectric properties should be conducted. Therefore, it is the aim of the present work to apply the Density Functional Theory (DFT) to investigate the structural, electronic, optical, elastic and thermoelectric properties of anti-perovskite nitrides of the form $Sr_3MN$ (M = P and As).

## 2. Computational Methods

In this study, we have conducted first-principles calculations within the framework of density functional theory (DFT) using the Quantum Espresso code (Paolo *et al.*, 2009). The exchange-correlation energy was treated with the generalized gradient approximation (Perdew *et al.*, 1996) and ultra-soft pseudo potentials. To optimize the geometry of the systems, the Broyden-Fletcher-Goldfarb-Shanno (BFGS) minimization procedure was employed. The wave function cutoff energy was set to 70 Ry for $Sr_3PN$ and $Sr_3AsN$. For the self-consistent field (SCF) and lattice optimization, a 5×5×5 k-point grid was used, with a convergence threshold of $10^{-8}\ eV$ for the total energy. The non-self-consistent field (NSCF) calculations for the density of states (DOS) and band structure utilized a 8 × 8 × 8 k-point grid. The Thermo-pw package was utilized to investigate the elastic and optical properties, employing the Voigt-Reuss-Hill approximation for the elastic property calculations. To explore the thermoelectric properties, the Boltzmann transport formalism embedded in the BoltzTrap code was employed. A denser 15 ×15 ×15 k-point mesh was used to accurately sample the Brillouin Zone. The thermoelectric properties investigated included electrical conductivity ($\sigma/\tau$), Seebeck coefficient (S), thermal conductivity ($\kappa/\tau$), and figure of merit (ZT). The Fermi energy level in electron volts (eV)

served as the zero reference level. A relaxation time of $10^{-14}$ s, as suggested in the BoltzTrap manual, was utilized.

## 3. Results and Discussion

### *3.1 Structural Properties*

In their ideal structure, the anti-perovskites $Sr_3PN$ and $Sr_3AsN$ crystallize in a cubic structure with space group number 221 ($pm\bar{3}m$). The three Sr atoms occupy (1/2,0,1/2), (1/2,1/2,0) and (0,1/2,1/2) Wyckoff positions. Meanwhile, As or P atoms are located at Wyckoff coordinate of (0,0,0) whereas N atom occupies (1/2,1/2,1/2). The unit cell of the crystal is visualized in **Figure 1**.

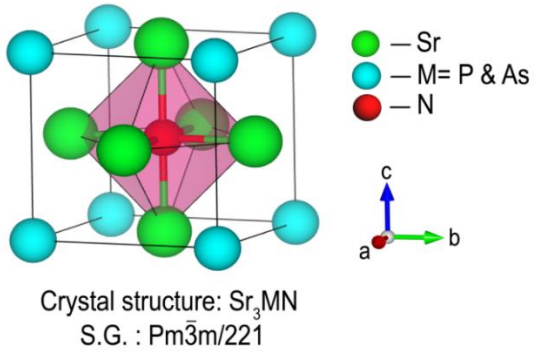


**Figure 1.** The unit cell of $Sr_3MN$ (M=P and As)

The optimization procedure has resulted in optimized lattice constants of $Sr_3MN$ (M=P and As), summarized in **Table 1**. Since the cubic structure of $Sr_3PN$ is reported for the first time in this study, its lattice parameter cannot be compared with other studies. Sreedevi et al (Sreedevi *et al.*, 2022) has studied this material but in its orthorhombic structure, where it was reported that a = 7.29 Å, b = 10.09 Å, and c = 7.05 Å. Meanwhile, there is a discrepancy found in the calculated lattice constant of the $Sr_3AsN$ anti-perovskite. Our calculated lattice constant of this compound (5.11 Å) agrees very well with that obtained using GGA-PBE reported in (Haque and Hossain, 2019) (5.13 Å) and (Ullah *et al.*, 2016; Hichour *et al.*, 2010) (5.12 Å). On the other hand, a quite large discrepancy is observed between our result and that of (Beznosikov, 2003) (5.03 Å) and (Ullah *et al.*, 2016) (5.05 Å). This discrepancy can be resolved by future experimental studies on this compound.

**Table 1.** Optimized lattice constants ($a_0$) and formation energy of cubic anti-perovskites $Sr_3MN$ (M=P and As).

| **Compounds** | **$a_0$(Å): this study** | **$a_0$(Å): literature** | **Formation energy (eV/atom)** |
|---|---|---|---|
| $Sr_3PN$ | 5.07 | - | -4.32 |
| $Sr_3AsN$ | 5.11 | 5.13 (Haque and Hossain, 2019), 5.12 (Ullah *et al.*, 2016), 5.12 (Hichour *et al.*, 2010), 5.03 (Beznosikov, 2003), 5.05 (Ullah *et al.*, 2016). | -4.26 |

The formation energy $\Delta E_f$ of the anti-perovskites has been calculated using **Eqn. 1** to investigate their chemical and stability:

$$\Delta E_f = \frac{E_{tot}(Sr_3MN) - 3E(Sr) - E(M) - E(N)}{n} \qquad \textbf{Eqn. 1}$$

where $E_{tot}(Sr_3MN)$ is the total energy of the unit cell of the cubic $Sr_3MN$ anti-perovskites, E(Sr), E(M) and E(N) are the energy of Sr, M (M=As or P), and N atoms, respectively, while n is the number of atoms in the unit cell. As the calculated formation energies of the two compounds are negative, the two anti-perovskites are predicted to be chemically stable. The chemical and structural stability of cubic $Sr_3MN$ anti-perovskites have also been reported in the previous studies such as in Ref (Haque and Hossain, 2019), supporting our findings.

### *3.2 Electronic Properties*

The electronic properties of the cubic anti-perovskites $Sr_3MN$ (M=P and As) have been calculated using the GGA-PBE functional. The band structure of $Sr_3PN$ and $Sr_3AsN$ compounds are plotted and shown in **Figure 2 a & b**, respectively. As expected, the general feature of the electronic structure of the two compounds. Additionally, **Figure 2 a & b** clearly indicate that the two compounds are direct-gap semiconductors (Γ→Γ); with band gaps are predicted to be 0.56 eV for $Sr_3PN$ and 0.45 eV for $Sr_3AsN$ anti-perovskites. While the band gap energy of the cubic $Sr_3PN$ is reported for the first time in the present work, the band gap of the cubic $Sr_3AsN$ has already been calculated using a number of theoretical approaches. A comparison of our results with other theoretical results is presented in **Table 2**.

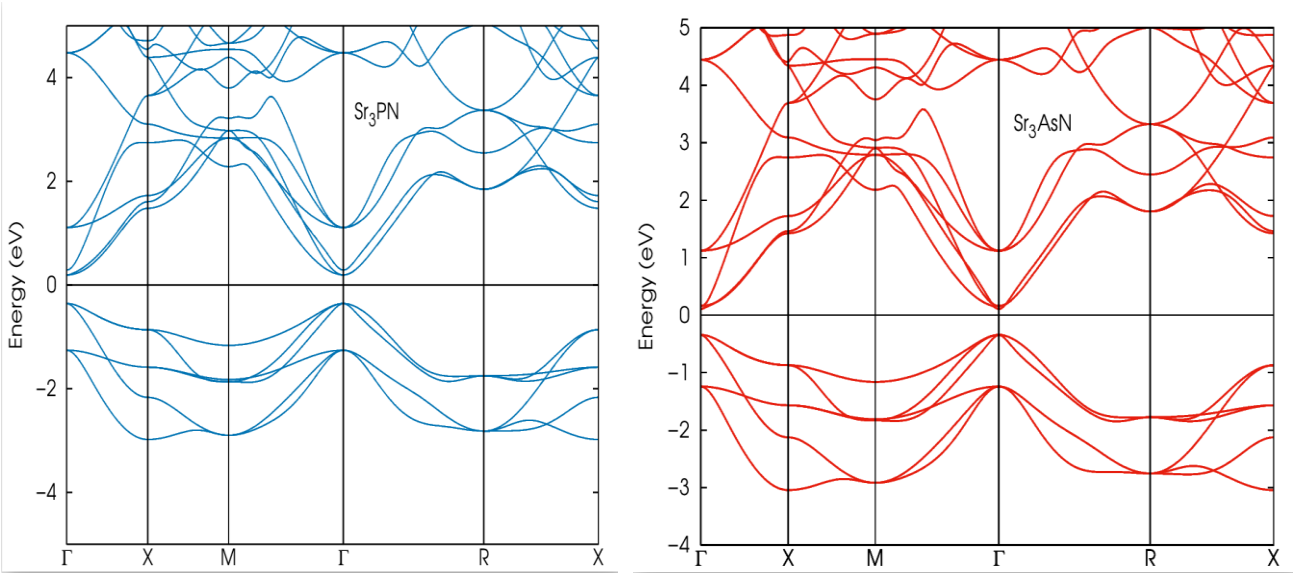


**Figure 2.** Electronic band structure of the cubic $Sr_3PN$ (**a**) and $Sr_3AsN$ (**b**).

**Table 2.** Calculated energy gap $E_g$ of cubic anti-perovskites $Sr_3AsN$, compared with other theoretical results in the literature

| ***$E_g$* (eV): this work: GGA-PBE** | ***$E_g$* (eV): literature** | **Approach used (literature)** |
|---|---|---|
| 0.45 (Γ→Γ) | 0.52 (Haque and Hossain, 2019) (Γ→Γ) | PBE |
| | 0.84 (Haque and Hossain, 2019) (Γ→Γ) | BJ |
| | 1.20 (Haque and Hossain, 2019) (Γ→Γ) | TB-mBJ |
| | 1.22 (Haque and Hossain, 2019) (Γ→Γ) | KTB-mBJ |
| | 1.24 (Haque and Hossain, 2019) (Γ→Γ) | nKTB-mBJ |
| | 0.38 (Hichour *et al.*, 2010) (Γ→Γ) | GGA |
| | 0.84 (Hichour *et al.*, 2010) (Γ→Γ) | GGA-eV |
| | 0.49 (Haddadi *et al.*, 2009) (Γ→Γ) | GGA |

It is not surprising that there are many theoretical studies performed to study the properties of $Sr_3AsN$ because the material has not been experimentally synthesized yet. From **Table 2**, all the

theoretical studies have reported that the material is a direct-gap semiconductor. It is also clear that the use of other approaches including BJ, TB-mBJ, KTB-mBJ, nKTB-mBJ eventually increases the band gap of the material. All these values will need to be verified experimentally.

### *3.3 Elastic properties*

The elastic properties of the two anti-perovskites are summarized in **Table 3**, where comparisons with other theoretical results in the literature are also presented wherever possible.

**Table 3.** Calculated elastic properties of cubic anti-perovskites $Sr_3PN$ and $Sr_3AsN$ using the GGA-PBE, compared with other theoretical results in the literature where available

| **Elastic properties** | **$Sr_3PN$** | | **$Sr_3AsN$** | |
|---|---|---|---|---|
| | **This work** | **Others** | **This work** | **Others** |
| Elastic const. $C_{11}(GPa)$ | 115.73 | - | 109.15 | **GGA:**95[†], 98.57[††], 110[†††]; **LDA**: 134[†††] |
| Elastic const. $C_{12}(GPa)$ | 16.05 | - | 16.71 | **GGA:**23[†], 14.78[††], 16.9[†††]; **LDA**: 18[†††] |
| Elastic const. $C_{44}(GPa)$ | 34.40 | - | 35.07 | **GGA:**29[†], 46.41[††], 35.8[†††]; **LDA**: 37[†††] |
| $B(GPa)$ | 49.27 | - | 47.52 | **GGA:**47[†], 42.71[††], 48[†††]; 47.44[††††]; **LDA**:57[†††] |
| $G(GPa)$ | 39.92 | - | 39.17 | **GGA:**45.5[††], 38.8[†††]; **LDA**: 44.3[†††] |
| $B/G\ (GPa)$ | 1.23 | - | 1.21 | 0.94[††], 1.24[†††]; **LDA**: 1.29[†††] |
| $E(GPa)$ | 95.51 | - | 92.18 | 99.2[††], 93.6[†††]; **LDA**: 105.5[†††] |
| $\nu$ | 0.18 | - | 0.176 | 0.11[††], 0.175[†††]; **LDA**: 0.19*** |
| A | 0.69 | - | 0.75 | 1.11[††], 0.77[†††]; **LDA**: 0.64[†††] |

[†](Haque and Hossain, 2019); [††](Hichour *et al.*, 2010); [†††](Haddadi *et al.*, 2009); [††††](Ullah *et al.*, 2016).

To the best of our knowledge, calculations on elastic properties of the cubic $Sr_3PN$ have not been reported. On the other hand, a number of theoretical studies have reported the elastic properties of the cubic $Sr_3AsN$. One of the most important elastic properties of materials is their mechanical stability, which can be analyzed from their elastic constants. The Born-Huang mechanical stability criteria (Born, 1940), i.e. $C_{11} > 0$, $C_{44} > 0$, $(C_{11}-C_{12}) > 0$, $(C_{11}+2C_{12}) > 0$, and $C_{12} < B < C_{11}$, were applied to evaluate the mechanical stability of the two anti-perovskites. The calculated elastic constants of the cubic anti-perovskites $Sr_3PN$ and $Sr_3AsN$, as presented in **Table 3**, meet these Born-Huang criteria and therefore they are mechanically stable. This has also been predicted for the cubic $Sr_3AsN$ by a number of previous investigations (Haque and Hossain, 2019; Hichour *et al.*, 2010; Haddadi *et al.*, 2009).

It is predicted that $Sr_3PN$ has higher bulk modulus (49.27 GPa) than $Sr_3AsN$ anti-perovskite (47.52 GPa), indicating that the anti-perovskite $Sr_3PN$ is more resistant to external pressure than $Sr_3AsN$. Similarly, $Sr_3PN$ also exhibits stronger shear resistance than $Sr_3AsN$, as seen from their shear modulus G. In addition, from their Young modulus, the cubic $Sr_3PN$ is also expected to be stiffer that $Sr_3AsN$. Furthermore, materials are ductile if their Poisson ratio is larger than 0.26 and are brittle otherwise (Ghaithan *et al.*, 2021). Based on the calculated Poisson ratio ν in **Table 3**, it can be inferred that both $Sr_3PN$ and $Sr_3AsN$ anti-perovskites have brittle behavior. This is also supported by their

Pugh's ratio (Pugh, 1954) which is smaller than 1.75, confirming their brittle behavior. As for the anisotropy factor A, representing the extent of single crystal anisotropy, our results indicate that the two anti-perovskites have relatively considerable degree of anisotropy. **Table 3** also shows that our calculated elastic properties of the cubic $Sr_3AsN$ agree very well with other theoretical results, especially those using the GGA approaches. The GGA results of (Haddadi *et al.*, 2009), in particular, are in excellent agreement with ours for all elastic properties considered. This is an indication that our results are a reliable prediction of the elastic properties of $Sr_3AsN$ and this should apply for the cubic $Sr_3PN$ anti-perovskite, which has not been previously studied.

### *3.4 Optical properties*

The real part of the dielectric function $\varepsilon_1(\omega)$ as a function of photon frequency ω and its imaginary part $\varepsilon_2(\omega)$ have been computed and the results are illustrated in **Figure 3a-b**, respectively.

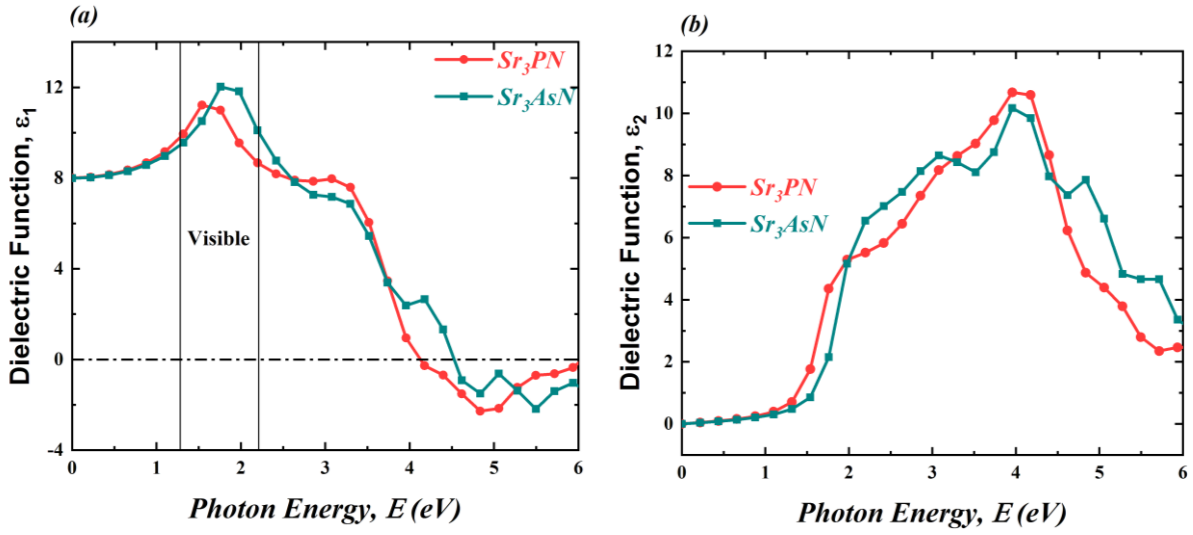


**Figure 3.** Real dielectric function $\varepsilon_1(\omega)$ (a) and imaginary dielectric function $\varepsilon_2(\omega)$ (b) of the cubic $Sr_3PN$ and $Sr_3AsN$.

**Figure 3a** and **3b** clearly show that the general feature of the real and imaginary part of the two anti-perovskites is similar. The static dielectric constants $\varepsilon_1(0)$ of $Sr_3PN$ and $Sr_3AsN$ are found to be 8.00 and 7.99, respectively. The real dielectric constants $\varepsilon_1(\omega)$ of the two materials then increase and reach their highest peaks in visible energy range, as illustrated in **Figure 3a**. These values then decrease and reach negative values at 4.17 eV and 4.62 eV for the respective compounds, and remain negative up to 6 eV. **Figure 3b** visualizes the imaginary part of the dielectric functions $\varepsilon_2(\omega)$, which describes the absorption behavior of the compounds. As seen from the figure, the corresponding values for the two compounds tend to increase and reach the maximum values of 10.68 for $Sr_3PN$ and 10.17 for $Sr_3AsN$, both appearing at 3.96 eV. The $\varepsilon_2(\omega)$ values then experience a decrease towards 6 eV. These results agree very well with those reported by (Ullah *et al.*, 2016) on $Sr_3AsN$ anti-perovskite, which are also similar to those of a number of isoelectronic compounds including $Ca_3AsN$, $Ca_3SbN$, $Ca_3BiN$, $Sr_3SbN$, $Sr_3BiN$, $Ba_3AsN$, $Ba_3SbN$, and $Ba_3BiN$. Likewise, Farid and co-workers (Farid *et al.*, 2021) reported similar findings on the cubic and orthorhombic $Sr_3AsN$.

The computed dielectric functions were then used to compute other optical properties of the compounds namely the reflectivity R(ω), absorption coefficient α(ω), refractive index η(ω), and the extinction coefficient k(ω). The results of these properties as functions of the photon frequency ω in

the range [0,6] eV are illustrated in **Figure 4a**, **4b**, **4c**, and **4d**, respectively. In general, $Sr_3PN$ and $Sr_3AsN$ anti-perovskites have relatively low reflectivity (not exceeding 50%) across the whole energy range [0,6] eV, with the maximum values of reflectivity predicted to be 43.84% at 4.84 eV and 43.25% at 5.50 eV, for the respective compounds (see **Figure 4a**). The static reflectivity values R(0) of the two anti-perovskites are the same, i.e. 22.8%.

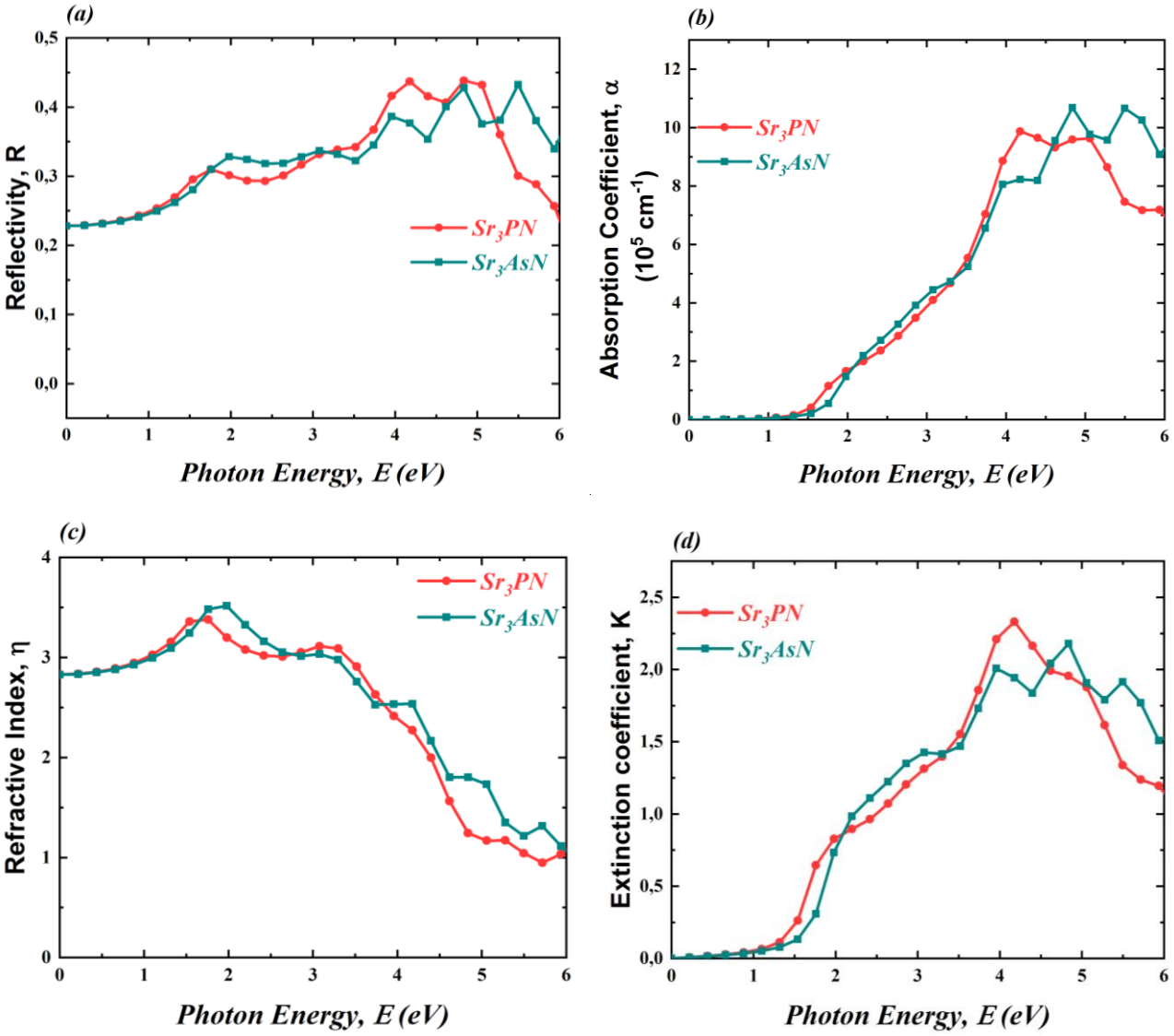


**Figure 4.** Reflectivity R(ω) (**a**), absorption coefficient α(ω) (**b**), refractive index η(ω) (**c**) and extinction coefficient k(ω) (**d**) of the cubic $Sr_3PN$ and $Sr_3AsN$.

The two materials are also predicted to show strong absorption within this energy range, in the order of $10^5$ $cm^{-1}$, as clearly seen in **Figure 4b**. This is also in agreement with the results reported in Refs (Farid *et al.*, 2021; Ullah *et al.*, 2016) for $Sr_3AsN$. The computed refractive index as a function of photon energy η(ω) can be seen in **Figure 4c**, where the static refractive index values η(0) of $Sr_3PN$ and $Sr_3AsN$ are the same (0.282). The general feature of this η(ω) curve is very similar to that of the real part of the dielectric constants $\varepsilon_1(\omega)$ (**Figure 3a**), as expected. Likewise, the general shape of the extinction coefficient k(ω) of the two compounds (Fig. 4d) closely resembles that of the imaginary part of the dielectric function $\varepsilon_2(\omega)$ (**Figure 3b**). The maximum extinction coefficients of $Sr_3PN$ and $Sr_3AsN$ are found at photon energies of 4.18 eV and 4.84 eV, respectively.

### *3.5 Thermoelectric properties*

The thermoelectric properties of the cubic $Sr_3PN$ and $Sr_3AsN$ anti-perovskites have been calculated in the range [0,800] K and the results are presented in this section. It is important to note that the properties of the cubic $Sr_3PN$ are reported for the first time in this study. The thermoelectric properties include the thermal conductivity over relaxation time ($\kappa/\tau$), the electrical conductivity over relaxation time ($\sigma/\tau$), the Seebeck coefficient (S), and the electronic figure of merit (ZTe), plotted in **Figure 5a**, **5b**, **5c**, and **5d**, respectively.

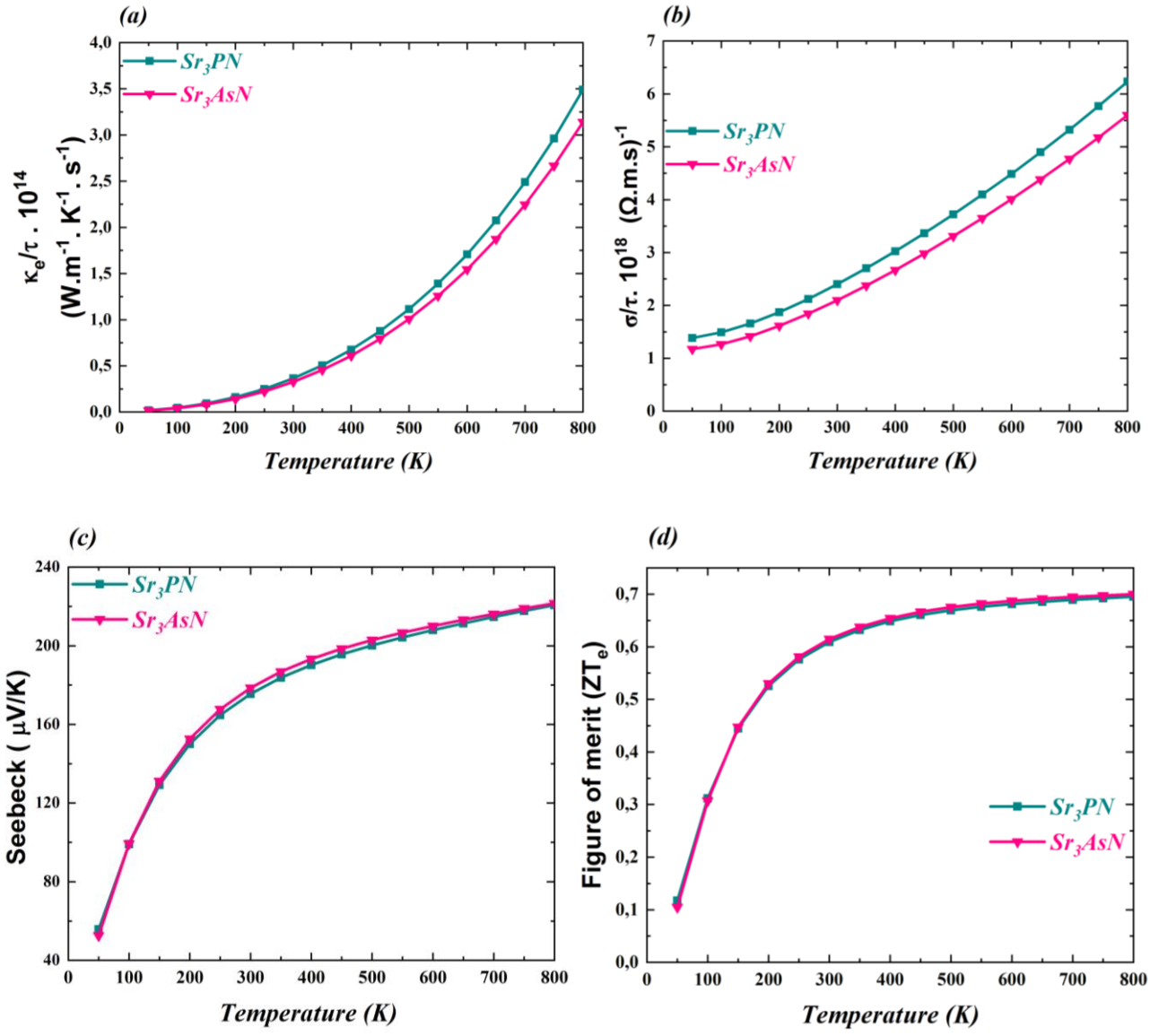


**Figure 5**. Electronic thermal conductivity (**a**), Electrical conductivity (**b**), Seebeck coefficient (**c**), and figure of merit (**d**) of the cubic $Sr_3PN$ and $Sr_3AsN$.

Heat conduction in materials is due to lattice vibrations and electronic contribution. In this study, because of the limitation of the BoltzTraP package, only the electronic contribution to the thermal conductivity ($\kappa_e$) of the compounds as a function of temperature was calculated and the results are presented in **Figure 5a**. It can be seen from the figure that at very low temperature, only a slight increase is observed but for larger temperature, it experiences a sharp increase and reaches its

maximum values at 800 K, i.e. $3.49 \times 10^{14}\ Wm^{-1}K^{-1}s^{-1}$ for $Sr_3PN$ and $3.14 \times 10^{14}\ Wm^{-1}K^{-1}s^{-1}$ for $Sr_3AsN$. At room temperature, the predicted electronic thermal energy values of $Sr_3PN$ and $Sr_3AsN$ are $3.64 \times 10^{13}\ Wm^{-1}K^{-1}s^{-1}$ and $3.26 \times 10^{13}\ Wm^{-1}K^{-1}s^{-1}$, respectively. The trend in this electronic thermal energy has also been observed for the cubic and orthorhombic $Sr_3AsN$ and their isoelectronic such as $Mg_3AsN$, $Ca_3AsN$, and $Ba_3AsN$ (Farid *et al.*, 2021), within temperature range between 0 and 300 K. Moreover, similar feature was also predicted for $Ca_3SnO$ and $Sr_3SnO$ (Hassan *et al.*, 2018).

Similar to the electronic thermal conductivity, the electrical conductivity as shown in **Figure 5b** increases with the increase in the temperature for the entire temperature range [0,800] K, as expected. This is also consistent with the results reported in (Farid *et al.*, 2021) for $Sr_3AsN$ within energy range [0,300] K. On the other hand, Haque and Hossain (Haque and Hossain, 2019) predicted that the electrical conductivity of $Sr_3AsN$ increases sharply to reach a peak at about 550 K, and then slightly decreases.

**Figure 5c** illustrates the variation of the calculated Seebeck coefficients of the cubic $Sr_3PN$ and $Sr_3AsN$ anti-perovskites. As seen from the figure, the Seebeck coefficients of the compounds increase dramatically until about the room temperature and they then only experience a slight increase until 800 K. This significant rise in the Seebeck coefficient in the temperature range [0,300] K was also reported for $Sr_3AsN$ in (Farid *et al.*, 2021). Interestingly, the Seebeck coefficients of $Sr_3AsN$ are reported to decrease in the temperature range [200,700] K (Haque and Hossain, 2019). The positive Seebeck coefficients of $Sr_3PN$ and $Sr_3AsN$ anti-perovskites imply that the two materials are p-type semiconductors. The electronic Figure of merit (ZTe) is an important property to predict performance of promising thermoelectric materials (Mir and Gupta, 2021). In general, larger ZTe values correspond to better thermoelectric materials (Maughan *et al.*, 2016). Computed ZTe of $Sr_3PN$ and $Sr_3AsN$ is displayed in **Figure 5d**, where an increase in the ZTe values as a function of temperature is clearly seen. The most significant increase is observed between [0,300] K while only slight increase is found in higher temperature range. This trend is in good agreement with the results reported in (Haque and Hossain, 2019). It is also clear from **Figure 5d** that $Sr_3PN$ and $Sr_3AsN$ anti-perovskites are predicted to have almost the same performance as thermoelectric materials since they have almost the same ZTe values for the entire temperature range. At 800 K, the ZTe values of the two materials are predicted to be 0.70, slightly lower than the prediction of about 0.75 at 700 K (Haque and Hossain, 2019). This indicates that the two anti-perovskites are promising thermoelectric materials.

## Conclusion

The elastic, optoelectronic and thermoelectric properties of $Sr_3PN$ and $Sr_3AsN$ anti-perovskites have been successfully obtained and interpreted. Negative formation energy of the compounds implies their chemical stability and the evaluation of the elastic constants based on the Born-Huang stability criteria demonstrates their mechanical stability. The two compounds are predicted to have p-type semiconducting behavior with strong absorption in the visible and ultraviolet region, making them potential for optoelectronic applications. Finally, analysis of their thermoelectric properties suggests that they are promising thermoelectric materials.

**Acknowledgement:**

**Disclosure statement:** *Conflict of Interest:* The authors declare that there are no conflicts of interest.
*Compliance with Ethical Standards:* This article does not contain any studies involving human or animal subjects.

## References


D. Aman, D. R. Abd El-Hafiz, M. A. Ebiad (2018) Thermodynamic parameter for steam reforming reaction of biodiesel by-product using nano-sized perovskite catalysts, *Mor. J. Chem.* 6 N°3, 466-479 https://doi.org/10.48317/IMIST.PRSM/morjchem-v6i3.6444

Behera D., Dixit A., Nahak B., Srivastava A., Dubey S., Sharma R., Mishra A. K., Mukherjee S. K., (2022) Structural, electronic, elastic, vibrational and thermodynamic properties of antiperovskites $Mg_3NX$ (X = Ge, Sn): A DFT study, *Phys. Lett. A.*, 453, 128478.

Behera D., Mukherjee S. K., (2022) Optoelectronics and transport phenomena in $Rb_2InBiX_6$ (X = Cl, Br) Compounds for Renewable Energy Applications: A DFT Insight, *Chemistry*, 4, 1044-1059.

Beznosikov B. V., (2003) Predicted Nitrides with an Antiperovskite Structure, *J. Struct. Chem*., 44, 885-888. https://doi.org/10.1023/B:JORY.0000029831.93738.b1

Born M., (1940) On the stability of crystal lattices, *Math. Proc. Camb. Phil. Soc*., 36(2), 160-172. https://doi.org/10.1017/S0305004100017138

Bouhmaidi S., Pingak R. K., Azouaoui A., Harbi A., Moutaabbid M., Setti L., (2023) Ab initio study of structural, elastic, electronic, optical and thermoelectric properties of cubic Ge-based fluoroperovskites $AGeF_3$ (A = K, Rb and Fr), *Solid State Commun.*, 369, 115206.

Bouhmaidi S., Azouaoui A., Benzakour N., Hourmatallah A., Setti L., (2022) First principles calculations on structural, electronic, elastic, optical, and thermoelectric properties of thallium based chloroperovskites $TlMCl_3$ (M=Zn and Cd), *Comput. Condens. Mater*., 33, e00756.

Bouhmaidi S., Marjaoui A., Talbi A., Zanouni M., Nouneh K., Setti L., (2022) A DFT study of electronic, optical and thermoelectric properties of Ge-halide perovskites $CsGeX_3$ (X=F, Cl and Br), *Comput. Condens. Mater*., 31, e00663.

Dahbi S., Tahiri N., El Bounagui O., Ez-Zahraouy H., (2022) Earth-abundant nontoxic ternary calcium nitrides inverse perovskites for single-junction solar cells: Ab-initio simulations, *Mater. Sci. Semicond. Process*., 150, 106959.

Farid H. M. T., Mera A., Al-Muhimeed T., AlObaid A. A., Albalawi H., Hegazy H. H., Ejaz S. R., Khosa R. Y., Mehmood S., Ali Z. (2021) Optoelectronic and thermoelectric properties of $A_3AsN$ (A = Mg, Ca, Sr and Ba) in cubic and orthorhombic phase, *J. Mater. Res. Technol.*, 13, 1485-1495.

Ghaithan H. M., Alahmed Z. A., Qaid S. M. H., Aldwayyan A. S. (2021) Density functional theory analysis of structural, electronic, and optical properties of mixed-halide orthorhombic inorganic perovskites, *ACS Omega*, 6, 30752-30761.

Haddadi K., Bouhemadou A., Louail L., Rahal F., Maabed S. (2009) Prediction study of the structural, elastic and electronic properties of $ANSr_3$ (A=As, Sb and Bi), *Comput. Mater. Sci*., 46(4), 881-886.

Haque E., Hossain M. A. (2019) DFT based study on structural stability and transport properties of $Sr_3AsN$: A potential thermoelectric material, *J. Mater. Res*., 34(15), 2635-2642.

Harbi A., Moutaabbid M., (2022) First-Principles Investigation of Structural, Elastic, Thermoelectric, Electronic, and Optical Properties of Ordered Double Perovskite $Ba_2MWO_6$ (M = Mg, Zn, and Cd), *J. Supercond. Nov. Magn*., 35, 3447-3456.

Harbi A., Moutaabbid H., Li Y., Renero-Lecuna C., Fialin M., Le Godec Y., Benmokhtar S., Moutaabbid M. (2019) The effect of cation disorder on magnetic properties of new double perovskites $La_2Ni_xCo_{1-x}MnO_6$ (x = 0.2–0.8), *J. Alloys Compd.*, 778, 105-114.

Harbi A., Moutaabbid M. (2022) Thermoelectric and optoelectronic properties of novel lead-free halide perovskites $CsRbTiX_6$ (X= I, Br and Cl) for photovoltaic applications, *Comput. Condens. Matter*., 32, e00733.

Hassan M., Shahid A., Mahmood Q. (2018) Structural, electronic, optical and thermoelectric investigations of antiperovskites $A_3SnO$ (A = Ca, Sr, Ba) using density functional theory, *Solid State Commun*., 270, 92-98.

Hichour M., Khenata R., Rached D., Hachemaoui M., Bouhemadou A., Reshak A. H., Semari F. (2010) FP-

APW+lo study of the elastic, electronic and optical properties for the cubic antiperovskite $ANSr_3$ (A=As, Sb and Bi) under pressure effect, *Physica B Condens. Matter*., 405(7), 1894-1900.

He B., Dong C., Yang L., Chen X., Ge L., Mu L., Shi Y. (2013) $CuNNi_3$: A new nitride superconductor with antiperovskite structure, *Supercond. Sci. Technol*., 26, 125015.

Ho-Baillie A. W. Y., Zheng J., Mahmud Md. A., Ma F-J., Green M. A. (2021) Recent progress and future prospects of perovskite tandem solar cells, *Appl. Phys. Rev*., 8, 041307.

Huang Y-T., Kavanagh S. R., Scanlon D. O., Walsh A., Hoye, R. L. Z. (2021) Perovskite-inspired materials for photovoltaics and beyond-from design to devices, *Nanotechnology*, 32(13), 132004.

Kadri A., Hiadsi S., Elchikh M., Bahlouli S. (2023) Investigation of structural, mechanical, dynamic stability and electronic properties of anti-perovskite nitrides $ANLa_3$ (A = Al, Ga): a DFT and DFPT studies, *Phys. Scr*., 98, 055931.

Li X., Zhang Y., Kang W., Yan Z., Shen Y., Huo J. (2023) Anti-perovskite nitrides and oxides: Properties and preparation, *Comput. Mater. Sci*., 225, 112188.

Liang Q-Q., Hu D-Y., Zhao X-H., Tang T-Y., Gao H-X., Wu S-Q., Tang Y-L. (2022) Predicting the structural, elastic, electronic, and optical properties of anti-perovskites $X_3SbP$ (X = Ca, Sr, Ba) via first-principles, *Chem. Phys. Lett*., 808, 140127.

Maughan A. E., Ganose A. M., Bordelon M. M., Miller E. M., Scanlon D. O., Neilson J. R. (2016) Defect tolerance to intolerance in the vacancy-ordered double perovskite semiconductors $Cs_2SnI_6$ and $Cs_2TeI_6$, *J. Am. Chem. Soc*., 138, 8453-8464.

Mir S. A., Gupta D. C. (2021) Scrutinizing the stability and exploring the dependence of thermoelectric properties on band structure of 3d-3d metal-based double perovskites $Ba_2FeNiO_6$ and $Ba_2CoNiO_6$, *Sci. Rep*., 11, 10506.

Mochizuki Y., Sung H-J., Takahashi A., Kumagai Y., Oba F. (2020) Theoretical exploration of mixed-anion antiperovskite semiconductors $M_3XN$ (M = Mg, Ca, Sr, Ba; X = P, As, Sb, Bi), *Phys. Rev. Mater*., 4(4), 044601.

Nguyen H., Dien V. K., Lin M. –F. (2022) Electronic and optical properties of $CsGeX_3$ (X=Cl, Br and I) compounds, *ACS Omega*, 7(29), 25210-25218.

Okamoto Y., Sakamaki A., Takenaka K. (2016) Thermoelectric properties of antiperovskite calcium oxides $Ca_3PbO$ and $Ca_3SnO$, *J. Appl. Phys*., 119, 205106.

Oudah M., Ikeda A., Hausmann J. N., Yonezawa S., Fukumoto T., Kobayashi S., Sato M., Maeno Y. (2016) Superconductivity in the antiperovskite dirac-metal oxide $Sr_{3-x}SnO$, *Nat. Commun*., 7, 13617.

Oyeniyi E. (2022) Electronic and optical properties of $Mg_3XN$ (X = P, As, Sb, Bi) antiperovskites: The GW/BSE approach, *Solid State Commun*., 355, 114927.

Paolo G., Stefano B., Nicola B., Matteo C., Roberto C., Carlo C., Davide C., Guido C., Matteo C., Ismaila D., Andrea D. C., Stefano de G., Stefano F., Guido F., Ralph G., Uwe G., Christos G., Anton K., Michele L., Layla M-S., Nicola M., Fransesco M., Riccardo M., Stefano P., Alfredo P., Lorenzo P., Carlo S., Sandro S., Gabriele S., Ari P. S., Alexander S., Paolo U., Renata M. W. (2009) QUANTUM ESPRESSO: a modular and open-source software project for quantum simulations of materials, *J. Phys: Condens. Matter*., 21(39), 395502.

Perdew J. P., Burke K., Ernzerhof M. (1996) Generalized gradient approximation made simple, *Phys. Rev. Lett*., 77, 3865.

Pingak R. K. (2022) A DFT study of structural and electronic properties of cubic thallium based fluoroperovskites $TlBF_3$ (B = Ge, Sn, Pb, Zn, Cd, Hg, Mg, Ca, Sr, Ba), *Comput. Condens. Mater*., 33, e00747.

Pingak R. K., Bouhmaidi S., Setti L., Pasangka B., Bernandus B., Sutaji H. I., Nitti F., Ndii M. Z. (2023) Structural, Electronic, Elastic, and Optical Properties of Cubic $BaLiX_3$ (X = F, Cl, Br, or I) Perovskites: An Ab-initio DFT Study, *Indones. J. Chem*., 23(3), 843-862.

Pingak R. K., Bouhmaidi S., Setti L. (2023) Investigation of structural, electronic, elastic and optical properties of Ge-halide perovskites $NaGeX_3$ (X = Cl, Br and I): A first-principles DFT study, *Physica B Condens.*

*Matter*., 663, 415003.
Pugh S. F., (1954) Relations between the elastic moduli and the plastic properties of polycrystalline pure metals, *The London, Edinburgh, and Dublin Philosophical Magazine and Journal of Science*, 45, 823-843.
Roknuzzaman Md., Ostrikov K., Wang H., Du A., Tesfamichael T. (2017) Towards lead-free perovskite photovoltaics and optoelectronics by ab-initio simulations, *Sci. Rep.*, 7, 14025.
Song X., Zhao Y., Wang X., Ni J., Meng S., Dai Z. (2023) Strong anharmonicity and high thermoelectric performance of cubic thallium-based fluoride perovskites $TlXF_3$ (X = Hg, Sn, Pb), *Phys. Chem. Chem. Phys*., 25, 5776-5784.
Song X., Wang J., Zhao Y., Ni J., Meng S., Dai Z. (2022) Extremely strong four-phonon scattering and ultra-low lattice thermal conductivity due to quartic anharmonicity in fluoride perovskites $XHgF_3$ (X = K, Rb), *Phys. Lett. A*., 456, 128550.
Sreedevi P. D., Vidya R., Ravindran P. (2022) Antiperovskite materials as promising candidates for efficient tandem photovoltaics: First-principles investigation, *Mater. Sci. Semicond. Process*., 147, 106727.
Ullah I., Murtaza G., Khenata R., Mahmood A., Muzzamil M., Amin N., Saleh M. (2016) Structural and Optoelectronic Properties of $X_3ZN$ (X = Ca, Sr, Ba; Z = As, Sb, Bi) Anti-Perovskite Compounds, *J. Electron. Mater*., 45, 3059-3068.
Zhang L., Wang B., Sun Y., Tong P., Fan J., Zhang C., Pi L., Zhang Y. (2012) Critical behavior in the antiperovskite ferromagnet $AlCMn_3$, *Phys. Rev. B*., 85, 104419.

(2023) ; https://revues.imist.ma/index.php/morjchem/index